

Čerenkov third-harmonic generation in $\chi^{(2)}$ nonlinear photonic crystal

Yan Sheng,^{1,a)} Wenjie Wang,^{1,2} Roy Shiloh,³ Vito Roppo,⁴ Yongfa Kong,² Ady Arie,³ and Wieslaw Krolikowski¹

¹Laser Physics Center, Research School of Physics and Engineering, Australian National University, Canberra ACT 0200, Australia

²School of Physics, Nankai University, Tianjin 300071, People's Republic of China

³School of Electrical Engineering, Faculty of Engineering, Tel-Aviv University, Tel-Aviv 69978, Israel

⁴Departament de Física i Enginyeria Nuclear, Universitat Politècnica de Catalunya, Rambla Sant Nebridi, 08222 Terrassa, Spain

(Received 11 April 2011; accepted 1 June 2011; published online 17 June 2011)

We report on the observation of Čerenkov emission of a third-harmonic frequency in a two-dimensional nonlinear photonic crystal, where the second-order nonlinearity $\chi^{(2)}$ is spatially modulated by the reversal of ferroelectric domains. We analyze both spatial and polarization properties of the emitted radiation and find the results in agreement with our theoretical predictions. © 2011 American Institute of Physics. [doi:10.1063/1.3602312]

When a charged particle travels faster than the speed of light in a dielectric, it can drive the medium to emit coherent light called Čerenkov radiation.¹ In this process, the molecules of the medium are polarized by the passing electromagnetic field of the particle and photons are emitted as these molecules restore themselves to equilibrium. Intense light propagating in a nonlinear optical crystal or waveguide can also create such an emission via a quadratic nonlinear process such as Čerenkov second-harmonic generation (SHG).^{2–8} In this nonlinear wave phenomenon, the incident wave induces oscillations of the electric dipoles in the atoms of the medium, which can be regarded as small antennas that radiate electromagnetic wave at the second-harmonic (SH) of the input frequency. The Čerenkov SHG is observable at a conical wave front defined by the cone angle $\theta_c = \cos^{-1}(v'/v)$, where v is the phase velocity of the polarization source and v' is the velocity of the radiation wave. It occurs as $v > v'$.

While the nonlinear Čerenkov radiation in optical medium closely resembles the classical radiation via relativistic charged particles, it has unique distinguishing features. In contrast to the classic Čerenkov radiation, where the high velocity particle serves as the only driven source, any intense light wave propagating in a optical quadratic medium can induce the nonlinear polarization in the medium. This means that once a Čerenkov SH 2ω is generated, it will contribute to the interaction leading to the nonlinear polarization that contains new frequency components such as 3ω and 4ω . These two terms, in theory, will lead to Čerenkov third-harmonic generation (THG) and fourth-harmonic generation if the polarization phase velocity v does exceed the velocity of the harmonic radiation v' . However, despite large body of works on frequency conversion,^{9–12} such spatial emission of new frequencies has not been observed so far. Although a recent paper claimed observation of a noncollinear THG in a waveguide geometry¹³ that work deals in fact with a different process as the third-harmonic (TH) emission, involves an intermediate process of collinear SHG and relies on the automatically achieved phase matching (PM) between radiated and guided waves.

In this letter, we provide the experimental evidence of Čerenkov THG in a bulk $\chi^{(2)}$ nonlinear photonic crystal (NPC)¹⁴ with a spatial modulation of the second-order nonlinearity. We observe conical emission of a TH frequency when transversely illuminating the NPC. We show that the formation of such TH wave involves conservation of only longitudinal components of the momenta of the interacting waves and hence represents *cascaded* variant of the nonlinear Čerenkov radiation.

In experiment, we fabricated a two-dimensional short-range ordered NPC (SRO-NPC)^{15,16} via standard electric-field poling¹⁷ of a Z-cut LiNbO₃ wafer at room temperature. The dimensions of the poled crystal were 13.5 mm(x) × 20.9 mm(y) × 0.4 mm(z). The domain-inverted structure visualized by a scanning SHG microscopy¹⁸ is shown in Fig. 1(a). The inset illustrates the creation of the SRO structure by placing randomly rotated basic units on a square lattice with a period $b = 19.8 \mu\text{m}$. The basic units themselves are also squares with side length of $a = 8.5 \mu\text{m}$. The average diameter of the inverted domain was $5.5 \mu\text{m}$. The experimental setup for the Čerenkov harmonic generation is schematically shown in Fig. 1(b). As a light source, we used an optical parametric amplifier (Topas) generating 150 femtosecond pulses (250 Hz rep. rate) at $1.5 \mu\text{m}$ (full width at half maximum = 5.8 nm). The laser beam propagated along the z -axis of the sample and was focused by a lens that produced a focal spot with a diameter of $150 \mu\text{m}$. For a given input power, this beam size corresponded to an intensity of about 60 GW/cm^2 .

We observe that the transverse illumination of the SRO-NPC by the fundamental beam leads to simultaneous conical emission of the SH and TH waves. These waves form red ($\lambda = 750 \text{ nm}$) and green ($\lambda = 500 \text{ nm}$) rings in the far field [see Fig. 1(c)]. The measured cone angle for the SH radiation is $\theta_2 = 26^\circ$, which satisfies exactly the Čerenkov relation for SHG (Refs. 3 and 4), $k_2 \cos \theta_2 = 2k_1$. For LiNbO₃ crystal,¹⁹ this leads to the radiation of conical SH wave at external angle of $\theta_{2o}^{xt} = 26.11^\circ$ for ordinary and $\theta_{2e}^{xt} = 24.97^\circ$ for extraordinary waves. The observation of the conical TH ring in $\chi^{(2)}$ NPC was rarely reported elsewhere. It is a result of two-step cascading effect involving the successive SHG ($\omega_1 + \omega_1 = \omega_2$) and a sum frequency mixing (SFM,

^{a)}Electronic mail: ysh111@physics.anu.edu.au.

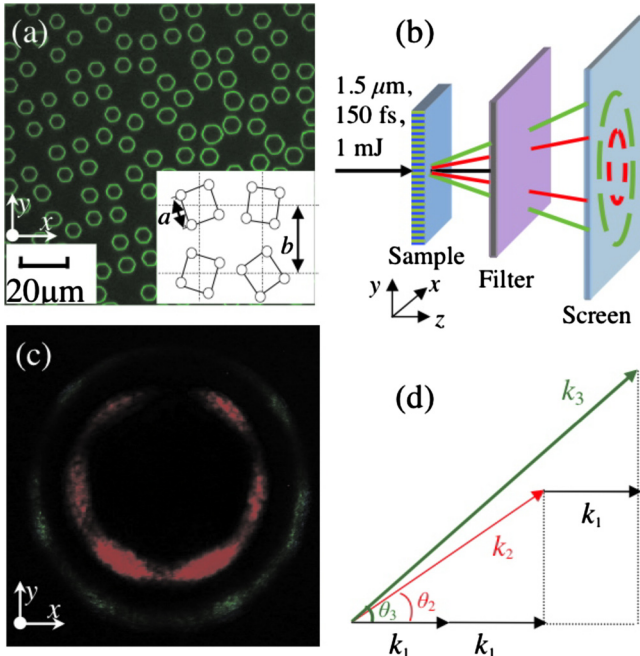


FIG. 1. (Color online) (a) The domain pattern imaged by the scanning SHG microscopy with the inset illustrating the creation of the structure. (b) Schematic of the experiment. (c) The observed Čerenkov SH and TH rings. The fundamental wave is linearly polarized along x -axis ($\gamma=0$). (d) The PM diagram of Čerenkov THG.

$\omega_1 + \omega_2 = \omega_3$). As was verified in the experiment, the measured propagation angle of this TH in air, $\theta_3 = 45^\circ (\pm 2^\circ)$, agrees well with that predicted by the cascading of two parametric processes that are only longitudinally phase-matched.

To understand the THG, we consider the PM conditions for the $\chi^{(2)}$ cascading process

$$\mathbf{k}_2 = 2\mathbf{k}_1 + \Delta\mathbf{k}_1, \quad (1)$$

$$\mathbf{k}_3 = \mathbf{k}_1 + \mathbf{k}_2 + \Delta\mathbf{k}_2, \quad (2)$$

where $\Delta\mathbf{k}_1$ and $\Delta\mathbf{k}_2$ are phase mismatches of the SHG and SFM processes, respectively. The nonlinear interactions occur most efficiently when the corresponding phase mismatch is zero. However, it is known that the strong nonlinear process is also possible in the Čerenkov scheme satisfying only the longitudinal PM condition. For the process of frequency tripling one obtains the longitudinal PM condition as [see Fig. 1(d)]:

$$k_3 \cos \theta_3 = k_1 + k_2 \cos \theta_2 = 3k_1. \quad (3)$$

The frequency tripling process governed by the scalar relation of Eq. (3) can be regarded as a Čerenkov-type THG since it relies only on the fulfillment of the longitudinal PM condition. The internal emission angle of the Čerenkov THG is determined only by the ratio of the refractive indices of the fundamental and TH waves as $\theta_3 = \cos^{-1}(n_1/n_3)$. For our case, this leads to external emission angle of $\theta_{3o}^{xt} = 48.61^\circ$ for ordinary and $\theta_{3e}^{xt} = 45.75^\circ$ for extraordinary TH waves, respectively. These values agree with the experimental results.

It is worth noting that the TH signal (green) was much weaker (~ 60 times) than the SH, so we had to use a very high gain of the charge coupled device camera to make these two rings clearly visible on a single picture. This led to slight oversaturation of the SH signal and therefore the width of the red and green rings in the figure does not represent the actual

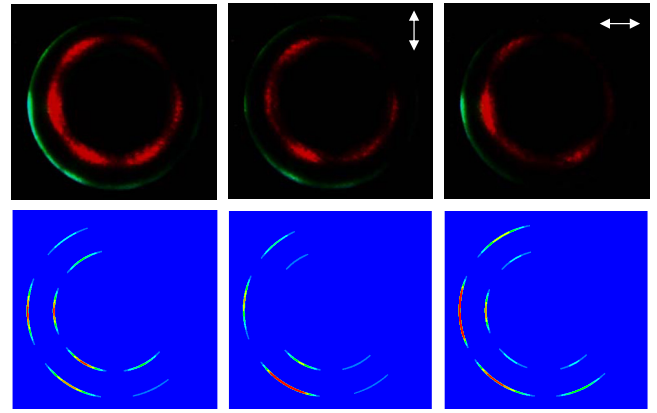


FIG. 2. (Color online) Experimentally recorded (top row) and theoretically predicted (bottom row) Čerenkov harmonic rings without analyzer with vertical analyzer and with horizontal analyzer (from left to right). The polarization angle of the fundamental wave is $\gamma = 30^\circ$.

angular spread of both harmonics. The attempts to observe the Čerenkov rings from single domain crystals using intensities up to the damage threshold failed. It is seen that the Čerenkov emissions are enhanced by the $\chi^{(2)}$ modulation. The physical reason of such enhancement is related to the presence of reciprocal vectors introduced by the modulation as well as modification of the nonlinearity itself in the region of domain wall.^{5,18} On the other hand, we have also observed THG Čerenkov rings in another LiTaO₃ crystal with a circular periodic domain reversal structures.

The Čerenkov harmonic rings are elliptically polarized because the ordinary and extraordinary waves are overlapped at each azimuthal angle. In fact, these two sets of rings can be spatially separated when projected onto a screen farther away from the sample. However, in this case the TH rings become rather vague as the beam has a large divergence angle. In order to record the TH rings more clearly here we used a lens to focus the harmonic beams such that the TH rings displayed in Fig. 2 appear thinner but brighter than that in Fig. 1(c). In the top row of Fig. 3, we show the Čerenkov THG recorded for several angles of input polarization. It is seen that the positions of the maximal intensity of the harmonic rings depend on the orientation of the input polarization.

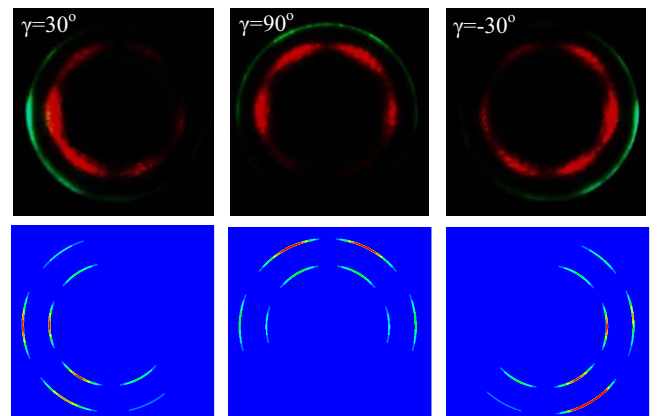


FIG. 3. (Color online) Experimentally recorded (top row) and theoretically predicted (bottom row) Čerenkov harmonic rings for different polarization angles of the fundamental wave. From left to right: $\gamma = 90^\circ$, 30° , and -30° , respectively.

The interesting polarization properties of the Čerenkov TH ring is determined by the structure of the $\chi^{(2)}$ tensor of the crystal, which can be explained by considering the concept of effective quadratic nonlinearity. The LiNbO₃ crystal belongs to $3m$ symmetry point group. For the fundamental wave propagating along the z -axis of the crystal, the following nonzero components are relevant: $d_{21}=-d_{22}$, $d_{31}=d_{32}$, and $d_{24}=d_{15}$. Then the effective nonlinearities of the frequency tripling process can be written as

$$d_{3o} = d_{32}A \sin \theta_2 \sin \xi - d_{22}(A \cos \theta_2 \cos \psi - B \sin \psi), \quad (4)$$

$$d_{3e} = d_{32}[B \sin \theta_3 \sin \xi - A \sin(\theta_2 + \theta_3) \cos \xi] - d_{22} \cos \theta_3(A \cos \theta_2 \sin \psi + B \cos \psi), \quad (5)$$

where θ_2 and θ_3 are the internal propagation angles of SH and TH wave, φ is the azimuthal angle, and γ is the angle defining the polarization of the fundamental beam. Finally, $\xi = \varphi - \gamma$, $\psi = 2\varphi + \gamma$, $A = d_{22} \sin \psi \cos \theta_2 + d_{32} \sin \theta_2$, and $B = d_{22} \cos \psi$ denote the effective nonlinearity of the SHG.^{3,4} Considering the fact that the ordinary and extraordinary harmonic waves spatially overlap in our case, the intensity of the Čerenkov SH and TH rings can be described by

$$I_2 \propto (S_{2o}B)^2 + (S_{2e}A)^2,$$

$$I_3 \propto (S_{3o}S_{2o}d_{3o})^2 + (S_{3e}S_{2e}d_{3e})^2, \quad (6)$$

where $S_{3o,3e} = \sin(\Delta k_{2o,2e}L/2)/(\Delta k_{2o,2e}L/2)$ and $S_{2o,2e} = \sin(\Delta k_{1o,1e}L/2)/(\Delta k_{1o,1e}L/2)$. Using Eq. (6), we calculated the azimuthal intensity distribution of the Čerenkov harmonic rings with different orientations of the analyzer and for different polarization angles of the fundamental wave (γ). We used the ratio of the two components of $\chi^{(2)}$ tensor $d_{32}/d_{22} = -3.9$.²⁰ The calculation results are shown in the bottom rows of Figs. 2 and 3 with the intensity distributions of both rings being normalized to their maximum intensities. It is seen the agreement between the experiment and theoretic results is quite good.

As follows from the figures, the Čerenkov harmonic rings exhibit an additional azimuthal intensity modulation with six well-defined peaks. As we have demonstrated previously,¹⁰ the appearance of such peaks cannot be explained using the effective nonlinearity but is associated only

with the hexagonally deformed ferroelectric domain.²¹ In the simulations shown above, we have already included such effect of the sixfold modulation.

In conclusion, we have studied the Čerenkov THG in $\chi^{(2)}$ NPC. We have analyzed both spatial and polarization properties of the emitted radiation. Our results are relevant for applications in three-dimensional ferroelectric domain visualization and the nonlinear microscopy.¹⁸ Moreover, the effects studied here are not limited only to nonlinear optics, and may be observed in other types of nonlinear physical systems, including, e.g., high intensity acoustic waves in solids.

The authors acknowledge the financial supports from Australian Research Council and Israeli Science Foundation (Grant No. 774/09).

¹P. A. Čerenkov, Dokl. Akad. Nauk SSSR **2**, 451 (1934).

²A. Zembrod, H. Puell, and J. Giordmaine, *Opt. Quantum Electron.* **1**, 64 (1969).

³S. M. Saltiel, D. N. Neshev, W. Krolikowski, R. Fisher, A. Arie, and Y. S. Kivshar, *Phys. Rev. Lett.* **100**, 103902 (2008).

⁴Y. Sheng, S. M. Saltiel, W. Krolikowski, A. Arie, K. Koynov, and Y. Kivshar, *Opt. Lett.* **35**, 1317 (2010).

⁵A. Fragemann, V. Pasiskevicius, and F. Laurell, *Appl. Phys. Lett.* **85**, 375 (2004).

⁶P. Molina, M. O. Ramirez, B. J. Garcia, and L. E. Bausa, *Appl. Phys. Lett.* **96**, 261111 (2010).

⁷X. Deng and X. Chen, *Opt. Express* **18**, 15597 (2010).

⁸Y. Zhang, Z. D. Gao, Z. Qi, S. N. Zhu, and N. B. Ming, *Phys. Rev. Lett.* **100**, 163904 (2008).

⁹V. Berger, *Phys. Rev. Lett.* **81**, 4136 (1998).

¹⁰S. M. Saltiel, Y. Sheng, N. Voloch-Bloch, D. N. Neshev, W. Krolikowski, A. Arie, K. Koynov, and Y. S. Kivshar, *IEEE J. Quantum Electron.* **45**, 1465 (2009).

¹¹C. Conti, E. D'Asaro, S. Stivala, A. Busacca, and G. Assanto, *Opt. Lett.* **35**, 3760 (2010).

¹²R. Sowade, I. Breunig, I. C. Mayorga, J. Kiessling, C. Tulea, V. Dierolf, and K. Buse, *Opt. Express* **17**, 22303 (2009).

¹³C. Chen, J. Lu, Y. Liu, X. Hu, L. Zhao, Y. Zhang, G. Zhao, Y. Yuan, and S. Zhu, *Opt. Lett.* **36**, 1227 (2011).

¹⁴A. Arie and N. Voloch, *Laser Photonics Rev.* **4**, 355 (2010).

¹⁵Y. Sheng, J. Dou, B. Ma, B. Cheng, and D. Zhang, *Appl. Phys. Lett.* **91**, 011101 (2007).

¹⁶Y. Sheng, S. M. Saltiel, and K. Koynov, *Opt. Lett.* **34**, 656 (2009).

¹⁷M. Houe and P. D. Townsend, *J. Phys. D* **28**, 1747 (1995).

¹⁸Y. Sheng, A. Best, H. Butt, W. Krolikowski, A. Arie, and K. Koynov, *Opt. Express* **18**, 16539 (2010).

¹⁹U. Schlarb and K. Betzler, *J. Appl. Phys.* **73**, 3472 (1993).

²⁰A. Ganany, A. Arie, and S. M. Saltiel, *Appl. Phys. B: Lasers Opt.* **85**, 97 (2006).

²¹Y. Sheng, T. Wang, B. Ma, B. Cheng, and D. Zhang, *Appl. Phys. Lett.* **88**, 041121 (2006).